Materials Science & Engineering B 254 (2020) 114516

Contents lists available at ScienceDirect

Materials Science & Engineering B

journal homepage: www.elsevier.com/locate/mseb

Graphene-zinc oxide nanocomposites (G-ZnO NCs): Synthesis, characterization and their photocatalytic degradation of dye molecules

Muthuchamy Maruthupandy[a,b,*], Pan Qin[a], Thillaichidambaram Muneeswaran[b], Govindan Rajivgandhi[c], Franck Quero[b], Ji-Ming Song[a,*]

[a] School of Chemistry & Chemical Engineering, AnHui Province Key Laboratory of Chemistry for Inorganic/Organic Hybrid Functionalized Materials, Anhui University, Hefei, Anhui 230601, PR China

[b] Laboratorio de Nanocelulosa y Biomateriales, Departamento de Ingeniería Química, Biotecnología y Materiales, Facultad de Ciencias Físicas y Matemáticas, Universidad de Chile, Avenida Beauchef 851, Santiago, Chile

[c] State Key Laboratory of Biocontrol and Guangdong Provincial Key Laboratory of Plant Resources, School of Life Sciences, Sun Yat-Sen University, Guangzhou 510275, PR China

ARTICLE INFO

Keywords:
Zinc oxide NPs
Graphene-zinc oxide nanocomposites
Photocatalytic degradation
Rhodamine-B
Methylene blue
Methyl orange

ABSTRACT

Highly pure zinc oxide nanoparticles (ZnO NPs) and graphene-zinc oxide nanocomposites (G-ZnO NCs) were synthesized via chemical precipitation method. The structure, morphology, and composition of the synthesized ZnO NPs and G-ZnO NCs were characterized by using fourier transfer infrared spectroscopy, X-ray diffraction spectroscopy, Raman spectroscopy, scanning electron microscopy and transmission electron microscopy (TEM). The TEM images revealed that the diameter of ZnO NPs is 8–12 nm and homogeneously dispersed onto the surface of graphene sheets. The photocatalytic degradation efficiency of the synthesized G-ZnO NCs against rhodamine-B (Rh-B), methylene blue (MB) and methyl orange (MO) was quantified under visible light irradiation. The irradiation time required for complete removal of the dyes are dependent on dye molecules (MB, MO and Rh-B) and their interaction with the prepared ZnO NPs and G-ZnO NCs. The synthesized NCs were highly efficient for the removal of Rh-B compared to other tested dyes. Hence, the synthesized G-ZnO NCs could be used for environmental dye remediation.

1. Introduction

In recent years, organic and inorganic dye molecules and their waste products from dye industries, along with fabric, paper and plastic have been seriously contaminating the environment [1]. Most of those dye molecules have excessive stability against light, temperature, chemical substances, and microbial action [2–4]. Photocatalytic degradation, however, has opened a brand new door for the removal of organic and inorganic dye molecules from water [5–7]. Photocatalytic degradation is based on the generation of electron hole pairs by the semiconductor photocatalyst including ZnO NPs and TiO_2 NPs, that absorbs light, exciting the electrons from valence band to conduction band [8].

The ZnO NPs are n-type and wide band hole (Eg = 3.37 eV) semiconductors used in numerous applications including nano-scale electronic and optoelectronic devices [9–11]. Due to its better photosensitivity and huge band gap , ZnO NPs have been considered as a promising photocatalyst alternative to TiO_2 NPs [12]. Several drawbacks, however, not limited to the excessive recombination rate of photogenerated electron–hole pairs, restrict the use of pure ZnO NPs for photocatalytic applications [10]. Consequently, to improve the photocatalytic performance, it is essential to gradually bring down the recombination of the charge carriers. Previously, the decrease of recombination rate was adressed by linking the photocatalysts with other substances including noble metals, semiconductors, and carbon materials was described [11].

Graphene, an atom-thick 2D layer nanomaterial is emerging as unique morphological carbon material with excellent electrical and mechanical properties [13]. These exciting properties make graphene a more extreme electron transport material for photocatalysis than C_{60} or graphite [14,15]. It has been shown that graphene mixed with nanoparticles such as TiO_2, ZnO, SnO_2 and CdS enhances photocatalytic reduction, improved performance in solar cells, and fuel cells [16]. As excited dye molecules can donate electrons to the conduction band of the semiconductor, it is usually possible that the excited dye molecules

* Corresponding authors at: School of Chemistry & Chemical Engineering, AnHui Province Key Laboratory of Chemistry for Inorganic/Organic Hybrid Functionalized Materials, Anhui University, Hefei, Anhui 230601, PR China.
E-mail address: jiming@ahu.edu.cn (J.-M. Song).

https://doi.org/10.1016/j.mseb.2020.114516
Received 9 February 2018; Received in revised form 19 November 2019; Accepted 3 March 2020
Available online 12 March 2020
0921-5107/

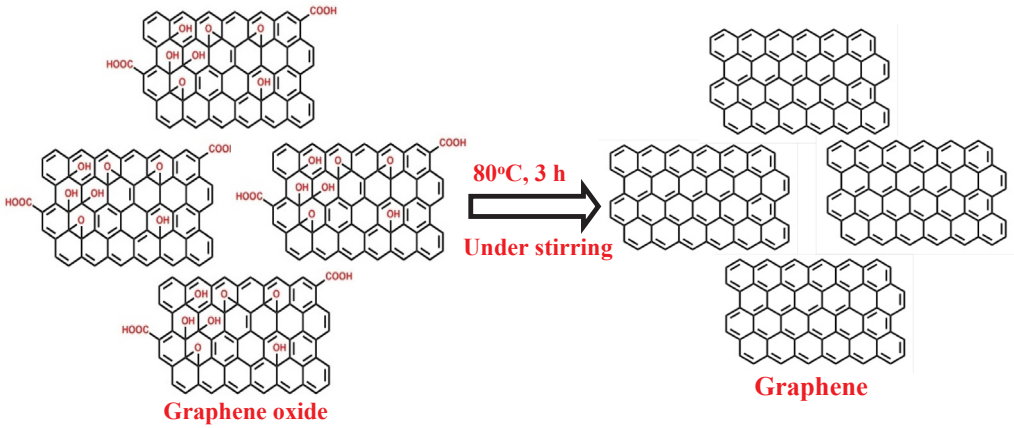

Scheme 1. Graphical representation of Graphene oxide converted to graphene using 80 °C, 3 h under constant stirring.

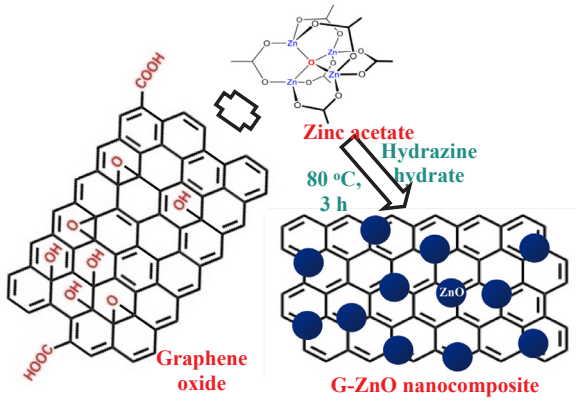

Scheme 2. Schematic demonstration of the fabrication of graphene-ZnO nanocomposite.

can introduce electrons to graphene or graphene derivatives for better redox reaction [17]. Since, graphene has excellent electron accepting property [17,18], it can be anticipated that the introduction of graphene will enhance the catalytic performance of the semiconductor.

Herring et al. [19] reported the photocatalytic activity of zinc oxide/graphene (GZ) nanocomposites prepared by microwave synthesis. Ahmad et al. [20] investigated the photocatalytic performance of solvothermally prepared GZ nanocomposites. Li et al. [1] synthesized flower-like ZnO nanoparticles decorated onto graphene (G) sheets and studied its photocatalytic degradation efficiency. Lv et al. [21] demonstrated photocatalytic degradation of methylene blue (MB) by ZnO–reduced GO (RGO)–carbon nanotube (CNT) synthesized by microwave-assisted method. Yang and Liu [22] reported graphene oxide/zinc oxide nanorods hybrid for potential multifunctional catalytic applications. One-step fabrication of macroscopic multifunctional graphene-based hydrogels with robust interconnected networks showed synergistic effects due to the reduction of graphene oxide sheets by ferrous ions and in situ simultaneous deposition of nanoparticles on graphene sheets [23]. However, to our knowledge, studies involving in-situ one step chemical synthesis of ZnO depositied onto graphene sheets (G-ZnO composite) are scarce [24,25]. In the present report, it was observed that the addition of graphene to ZnO NPs to form G-ZnO NCs has high impact on photocatalytic degradation and removal of dye molecules from water. The G-ZnO NCs presents remarkable catalytic degradation of rhodamine-B (Rh-B), methylene blue (MB) and methyl orange (MO) under visible light.

2. Material and methods

2.1. Materials

Graphite powder (99.95%) was purchased from Aladdin Industrial Corporation, China. 37 wt% hydrochloric acid (HCl), 98 wt% sulfuric acid (H_2SO_4), hydrogen peroxide (H_2O_2), potassium permanganate ($KMnO_4$), zinc acetate dihydrate ($Zn(CH_3COO)\cdot 2H_2O$), and hydrazine hydrate (N_2H_4) were purchased from Sinopharm Chemicals and Reagent Co. Ltd, China. All chemicals were used as received without further purification. Deionized (DI) water was used throughout this study.

2.2. Synthesis of ZnO nanoparticles

The ZnO NPs were synthesized by dissolving 0.2 M zinc acetate dihydrate ($Zn(CH_3COO)_2\cdot 2H_2O$) in 100 mL of water. Then, the solution was stirred for 3 h at room temperature to get transparent solution. 30 μL of hydrazine hydrate (N_2H_4) was added to the above solution and stirred at 80 °C for 3 h. The resulting precipitate was centrifuged and washed with DI water several times and dried. Finally, the powder was hardened at 450 °C for 4 h.

2.3. Synthesis of graphene oxide (GO)

Graphene oxide was synthesized by modified Hummer's method

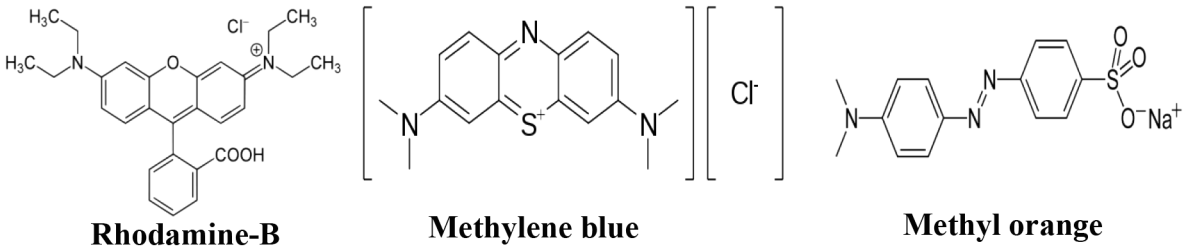

Scheme 3. Molecular structures of Rh-B, MB and MO dye molecules.

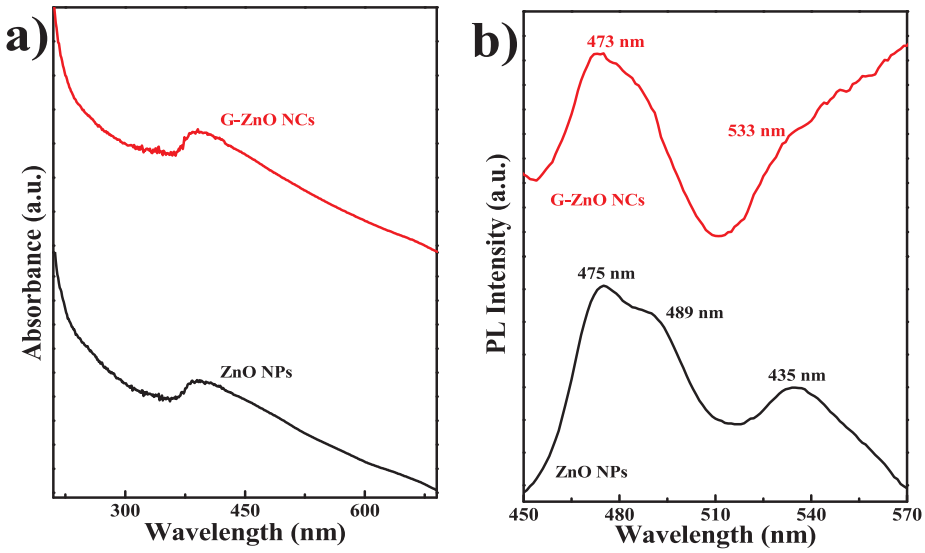

Fig. 1. UV–Visible absorption spectra (a) and PL spectra (b) of ZnO NPs and G-ZnO NCs.

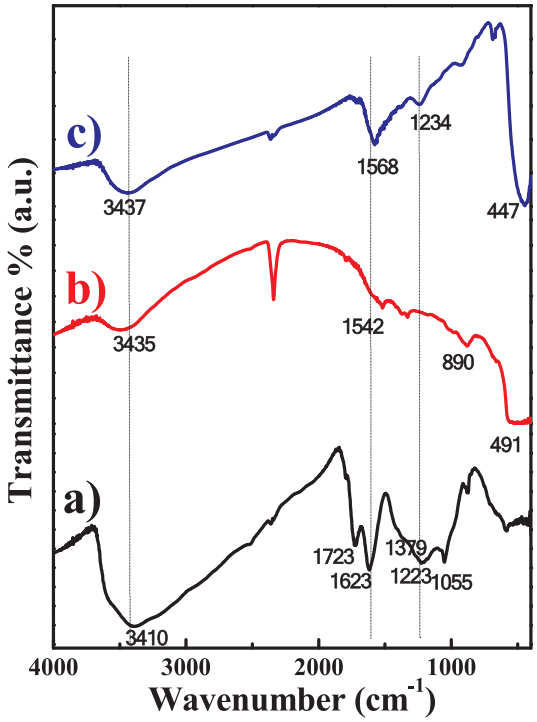

Fig. 2. FTIR spectra of (a) graphene, (b) ZnO NPs and (c) G-ZnO NCs.

[26]. Briefly, 1 g of graphite powder was added to 80 mL of H_2SO_4 (80 wt%) and stirred in an ice bath. After 30 min, 6 g of $KMnO_4$ was slowly added to the above solution and stirred. Then, the ice bath was replaced by an oil bath (30–35 °C) and the solution was stirred. After overnight in oil bath, 100 mL of water was slowly added and stirred for 30 min. A mixture of H_2O_2 (5 mL) and water (100 mL) was slowly added to the above solution and stirred for 10 min. The solution gradually turns from yellow to dark brown. The solution was then filtered to get the precipitate. The residue was initially washed (3–4 times) using HCl and then washed several times in DI water until neutral pH was reached .

2.4. Synthesis of G-ZnO NCs

Dried GO powder was dispersed in 90 mL of DI water (10 mg/mL) and sonicated for 30 min to obtain GO suspension. Subsequently, 300 mg of $Zn(CH_3COO)_2{\cdot}2H_2O$ was added to the GO suspension and stirred for 3 h. Then, 30 μL of hydrazine hydrate (N_2H_4) was added to the above solution and stirred for another 3 h at 80 °C. The solution turned from black to brown color, indicating the reduction of GO to graphene (Scheme 1). The precipitate was then centrifuged (3000 rpm) for 30 min and washed several times using DI water and alcohol. Later, the obtained powder was dried at 100 °C in an oil bath for 2 h and the dried powder heated for 4 h (Scheme 2) at 450 °C.

2.5. Characterization of ZnO NPs and G-ZnO NCs

Powder XRD of the synthesized samples was recorded by Rigaku D/max-RA X-ray diffractometer equipped with Cu-Ka radiation (λ = 1.54178 Å). The structural morphology and chemical elemental analysis of the samples were obtained using a scanning electron microscope (SEM, Hitachi S-4800) coupled with energy-dispersive X-ray spectroscopy (EDS). The surface morphology and size of the samples were investigated by transmission electron microscopy (TEM, Hitachi JEM-2100). Raman spectral measurements were performed at room temperature from 100 to 2000 cm^{-1} using a inVia Reflex Raman Microscope (Renishaw, United Kingdom). The room temperature photoluminescence (PL) was measured using a fluorimeter (FLSP920, Edinburgh Instruments, United Kingdom). UV–Vis absorption spectra were recorded using a spectrophotometer (Shimadzu UV-2450, Japan).

2.6. Photocatalytic activity

The photocatalytic properties of the prepared samples (ZnO NPs and G-ZnO NCs) towards MB, Rh-B and MO were quantified by UV–Vis spectrophotometer (Shimadzu UV-2450). In each experiment, 50 mg of photocatalyst, either ZnO NPs or G-ZnO NCs, was dispersed separately in 100 mL aqueous solutions containing MB, Rh-B and MO (1×10^{-5} M). The suspension was magnetically stirred in dark condition for 30 min. Later, the solution was transferred to flask and exposed to visible light irradiation at a regular time interval of 15 min. The absorption of the samples was recorded at respective peak maxima of 550, 660 and 450 nm for, respectively, Rh-B, MB and MO (Scheme 3).

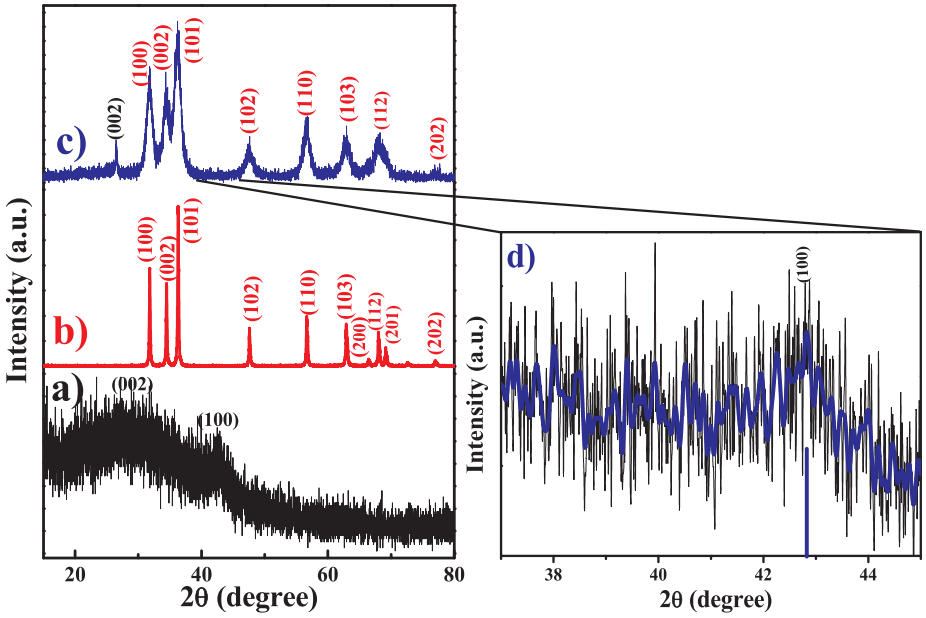

Fig. 3. Powder XRD patterns of (a) graphene, (b) ZnO NPs, (c) G-ZnO NCs and (d) high magnification pattern of G-ZnO NCs indicated the (1 0 0) plane of graphene.

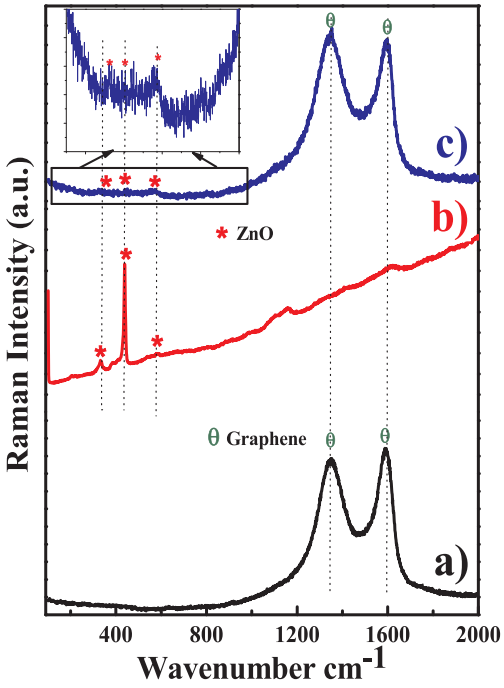

Fig. 4. Raman spectra of (a) graphene, (b) ZnO NPs (c) G-ZnO NCs.

3. Results and discussion

3.1. Characterization of ZnO NPs and G-ZnO NCs

The absorption property of ZnO NPs and G-ZnO NCs is reported in UV–Vis spectra in Fig. 1a). The ZnO NPs and G-ZnO NCs showed absorption peak in the UV region at ~389 nm and ~394 nm respectively, which is similar to the distinctive peaks of ZnO NPs and G-ZnO NCs reported by Jayabal et al. [25] and Azarang et al. [27]. In addition, G-ZnO NCs absorption peak was slightly shifted to red region from ~389 to ~394 nm due to ZnO NPs being coated onto graphene sheet. Hence, it is obvious that the addition of graphene is responsible for the little shift in band gaps. The PL spectra of the ZnO NPs and G-ZnO NCs at room temperature are displayed in Fig. 1b). The PL spectrum of pure ZnO NPs displays a distinct broad yellow-green emission peak in the 450–510 nm area with band central point at 470 nm, which is due to oxygen space in ZnO NPs arrangement [28]. The PL spectrum of G-ZnO NCs was, however, shifted to blue region from the peak observed for pure ZnO NPs. The ZnO NPs are good electron donor and graphene is an excellent electron acceptor; in composite, the electron movement between the conductivity band of ZnO NPs and graphene may responsible for the observed spectrum extinction [29]. From the result, it is concluded that the notable electron movement might decrease the recombination of photogenerated electron–hole pairs [30], and thus the synthesized G-ZnO NCs will display improved photocatalytic action compared to pure ZnO NPs.

The FTIR spectra of graphene, ZnO NPs and G-ZnO NCs are illustrated in Fig. 2a)–c). The spectrum of pure graphene (Fig. 2a)) showed FTIR features such as wide absorptions located at wavenumber positions of ~3410 and 1623 cm^{-1} owing to the vibrational motions of hydroxyl groups of H_2O molecules. The peaks located at wavenumber postions of ~1723 and 1055 cm^{-1} are assigned to the vibrational motions of C=O and C–O–C groups respectively, and the two peaks located at wavenumber positions of ~1379 and 1223 cm^{-1} are assigned to O–H vibrational motions of C–OH groups [31]. FTIR spectrum of the pure ZnO NPs (Fig. 2b)) showed, however, hydroxyl group vibrations at ~3435 and 1542 cm^{-1}. The strong absorption peak observed at a wavenumber of ~491 cm^{-1} is due to the vibrational motions of Zn–O [32]. When compared to the FTIR spectrum of graphene, G-ZnO NCs (Fig. 2c)) showed a slight shift with a decrease in the intensity of the O–H peak located at ~3437 cm^{-1}. However, the bands located at ~1723, 1379, and 1055 cm^{-1} related to C=O, O–H and C–O–C functional groups disappeared in G-ZnO NCs. This confirms the formation of ZnO NPs onto the surface of graphene following a partial reduction of the graphene [31,33]. Furthermore, the FTIR spectra of G-ZnO NCs, display an absorption band located at ~447 cm^{-1}, which corresponds to the E_2 vibrational mode of ZnO NPs [31]. For this reason, the synthesized NCs contain ZnO NPs adorned onto graphene sheet.

The XRD pattern of graphene, pure ZnO NPs, and G-ZnO NCs are shown in Fig. 3. In the XRD pattern of graphene, two extensive bands located at 2θ values of 26° and 42° were allotted to (0 0 2) and (1 0 0) planes of graphene, respectively (Fig. 3a)). The ZnO NPs XRD patterns in Fig. 3b) showed ten important peaks at the 2θ values of ~31°, 34°, 35°, 47°, 56°, 62°, 66°, 67°, 68° and 77° related to the crystal planes of

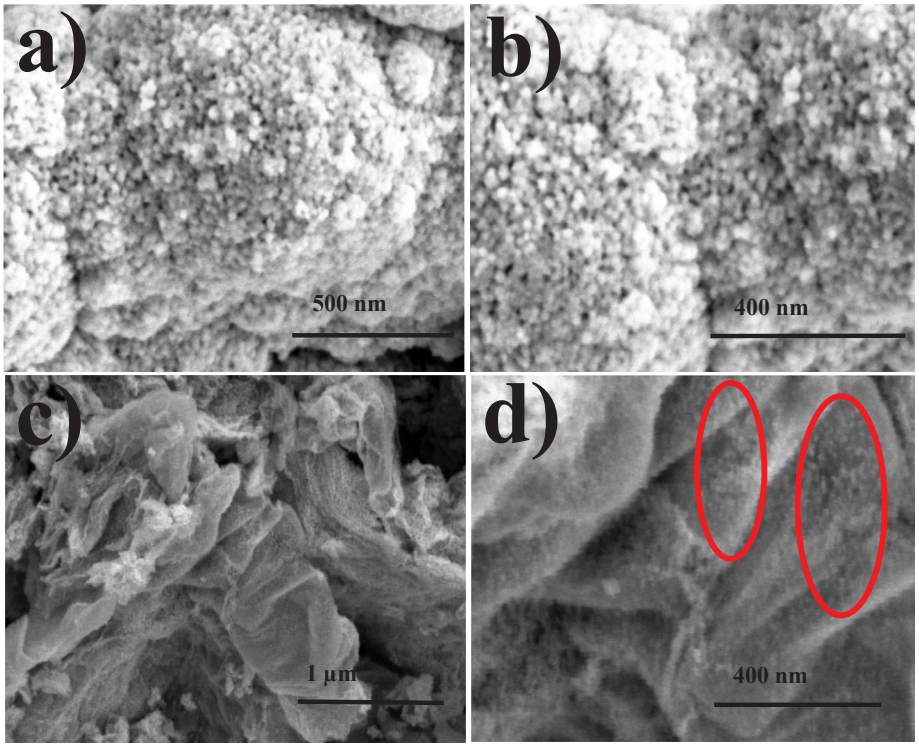

Fig. 5. Different magnification SEM images of ZnO NPs (a, b), G-ZnO NCs (c, d).

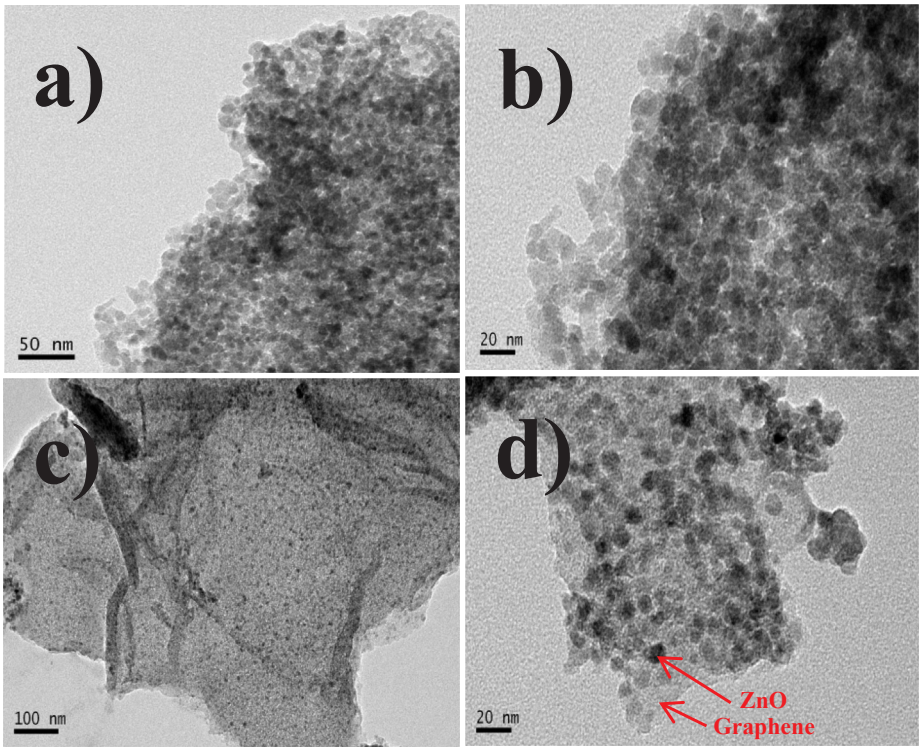

Fig. 6. Low and high magnification TEM images of ZnO NPs (a, b), G-ZnO NCs (c, d).

(1 0 0), (0 0 2), (1 0 1), (1 0 2), (1 1 0), (1 0 3), (2 0 0), (1 1 2), (2 0 1) and (2 0 2), respectively. The peaks of ZnO NPs observed in XRD pattern planes were in exact agreement with the JCPDS Card No: 36-1451 [25,34]. From the XRD pattern of G-ZnO NCs, it was obvious that the content of ZnO NPs is higher and the depth associated with ZnO NPs phase became larger [1]. A weak peak of graphene (0 0 2) at the 2θ value of ~26° observed in the XRD pattern of G-ZnO NCs confirms that the ZnO NPs were coated onto the surface of graphene (Fig. 3c)). The graphene (1 0 0) peak at 2θ value of ~42° in XRD of G-ZnO NCs was hindered (Fig. 3c)). This may be due to the presence of high ratio of ZnO NPs. However, by enlarging the XRD pattern of G-ZnO NCs, the peak at the 2θ value 42° related to the (1 0 0) plane of graphene could

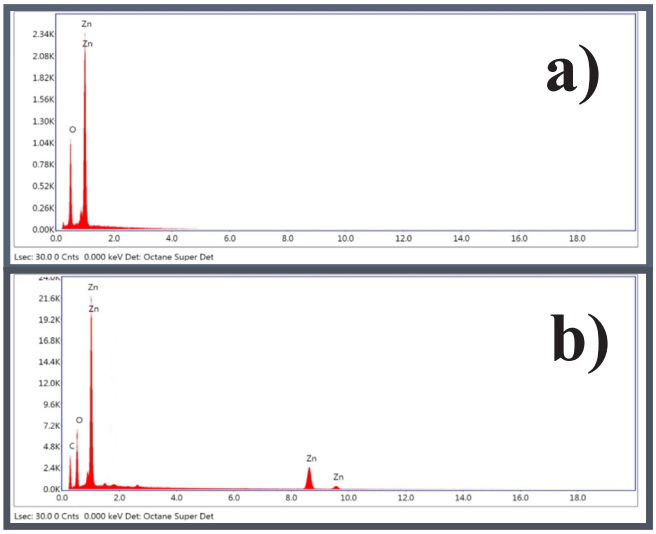

Fig. 7. EDX spectra of (a) ZnO NPs and (b) G-ZnO NCs.

be visualized Fig. 3d). This suggested that the ZnO NPs crowded over the graphene surface. The XRD patterns has distinct diffraction peaks of ZnO and graphene. confirming that the adopted method could synthesis NCs devoid of impurities.

Raman spectroscopy is one of the suitable method to qualify carbon based nanostructures [34]. Raman spectrum of graphene, ZnO and G-ZnO NCs are reported in Fig. 4. The Raman spectrum of ZnO NPs was found to be in regular Raman manner and the peaks were observed at ~330 (second-order vibration related to the E_2 (high)-E_2 (low)), 433 (E_2 (high)), and 582 cm^{-1} (E_1 (LO)) [5,25]. In Raman scattering, the backscattering geometry of ZnO NPs with spherical structure must show photons of the symmetry E_2 (high) at 433 cm^{-1} [35]. In the present study, the E_2 (high) way decided by the Raman spectrum of the synthesized ZnO NPs showed fabrication of wurtzite ZnO NPs as shown in Fig. 4b). The Raman spectrum of graphene shown in Fig. 4a) has two large peaks at ~1344 cm^{-1} (D band) and 1590 cm^{-1} (G band) indicate the drying condition of k-factor photons of A_{1g} symmetry and the primary order scattering of the E_{2g} phonon of sp^2 carbon atoms, respectively [36]. The D/G ratio (greater than the D/G ratio of graphene) indicate the existence of more morphological defects in the graphene arrangement elicited by the hydrazine hydrate aided reduction of graphene in the presence of ZnO NPs. This results in slightly aggregated ZnO NPs due to their strong interchange with defect sites of graphene sheets [19]. Fig. 4c) shows the Raman spectra of G-ZnO NCs and the G-ZnO NCs showed the ZnO peak, defect peak of D-band, and extensive deep G band. Since the concentration of ZnO NPs was higher, the intensity of E_2 mode has accrued. For this reason, the formation of wurtzite ZnO NPs and G-ZnO NCs could be confirmed through the Raman spectral analysis.

The morphology of ZnO NPs and G-ZnO NCs are displayed in Fig. 5. From the SEM images it is clearly visible that the ZnO NPs are spherical in shape and homogenously dispersed. The Fig. 5a) and b) showed that the ZnO particles are small and stick to one another. SEM images of G-ZnO NCs are shown in Fig. 5c) and d) showed that the individual ZnO NPs are stuck onto the surface of graphene sheets (highlighted of G-ZnO NCs) (Fig. 5d)). The SEM imagereported in Fig. 5c) display the shape of graphene sheet that was importantly exfoliated, and looks like part of flower with a dimension ranging from one hundred nm to several hundred nm. In addition, the Fig. 5d) shows the upper view of G-ZnO NCs confirms that ZnO NPs are decorated onto the surface of graphene sheets [32]. The ZnO NPs are stuck onto each surface of graphene sheets, which reduce the van der Waals forces among the graphene layers. Hence, the graphene sheets did not join together even after hardening [34].

Morphological differences between ZnO NPs and G-ZnO NCs were obtained from TEM and the images are displayed in Fig. 6. TEM images showed distinctly visible and uniformly distributed spherical like structure of ZnO NPs, which is portrayed in Fig. 6a), b). The TEM image under low magnification (Fig. 6c)) showed that ZnO NPs were decorated onto graphene sheets, whereas high magnification image (Fig. 6d)) showed that dense ZnO NPs were uniformly stick onto graphene sheet surface. In the present study, during the TEM sample preparation, G-ZnO NCs was subjected to sonication for a longer time. However, even after long sonication period, the ZnO NPs decorated onto the graphene sheet with a high density, which indicates the existence of strong interaction between ZnO NPs and graphene sheets.

The synthesized pure ZnO NPs and G-ZnO NCs were subjected to EDX analysis to establish and verify the chemical composition of the synthesized product and the results are shown in Fig. 7. The EDX spectrum of ZnO NPs shown in Fig. 7a) depicted that the NPs has 51.45 an atomic percent of Zn and 48.55% of O and the densely agglomerated region of the ZnO NPs. The G-ZnO NCs, however, has 50.46 atomic percentage of carbon (C), and 32.76% of Zn and 16.77% of O and the densely agglomerated region of the G-ZnO NCs are reported in Fig. 7b). The synthesized ZnO NPs and G-ZnO NCs is free from other elemental impurities and it consists of Zn, O, and C elements. Therefore, pure ZnO NPs and G-ZnO NCs can be synthesized through this one-step simple chemical technique.

3.2. Photocatalytic activity

The photocatalytic efficiency of the prepared ZnO NPS and G-ZnO NCs were tested against MB, MO and Rh-B dye molecules in aqueous solution as pollutant materials. The absorption of Rh-B, MB and MO dye molecules were in the visible region and their respective absorption maxima were 550, 660 and 450 nm. The time dependent UV–visible absorption spectra of MB, MO and Rh-B dye molecules in the presence of photocatalysts are displayed in Fig. 8. The intensity of the absorbance peak of Rh-B, MB and MO decreased upon increasing irradiation time. Furthermore, the time required to completely the removal of each dye molecule (MB, MO and Rh-B) differed for each dye, depending on the interaction of dye molecules with prepared ZnO NPs and G-ZnO NCs. The ZnO NPs and G-ZnO NCs interact differently with individual dye molecules such as Rh-B and MB, MO and the 100% degradation was reached at irradiation times of 180, 195, 195 min (Fig. 8a), c) and e)) and 90, 105, 120 min, respectively (Fig. 8b), d) and f)).

The photocatalytic degradation of MB, MO and Rh-B dye molecules in the presence of ZnO NPs and G-ZnO NCs under light irradiation is shown in Fig. 9. Compared to ZnO NPs the prepared G-ZnO NCs showed higher photocatalytic activity towards the tested dye molecules. Additionally, the photocatalytic effieciency of G-ZnO NCs was two times higher than that of the ZnO NPs. This is mainly due to the movement of electron motion from the conductivity band of ZnO NPs to graphene which may lower the recombination of photocreated electron–gap pairs. From the Fig. 9a) it is observed that the dye molecules samples degradation efficiency was in the order of Rh-B > MB = MO using ZnO NPs samples and Rh-B > MB > MO using G-ZnO NCs (Fig. 9b)). The dye molecule Rh-B could be easily degraded photo-catalytically compared to the other tested dyes.

Based on our result, we have discussed some of the works related to our studies, which were published elsewhere (Table 1). The photocatalytic degradation performance of ZnO–RGO nanocomposite against methylene blue (MB) was 88% within 260 min [21]. Nipane et al. [37] examined the degradation percentage of methylene blue (MB) and methyl orange (MO) and showed that after 90 min 99% of MB and 78% of MO removed in the presence of ZnO-RGO composites. The MB dye molecules in aqueous solution was degraded at 63 and 99.5% after 130 min using ZnO and ZnO-RGO composites [38]. Omar et al. [39] demonstrated that the MB dye molecules partly degraded (58.7%) within 80 min under the photocatalytic action of ZnO NPs whereas

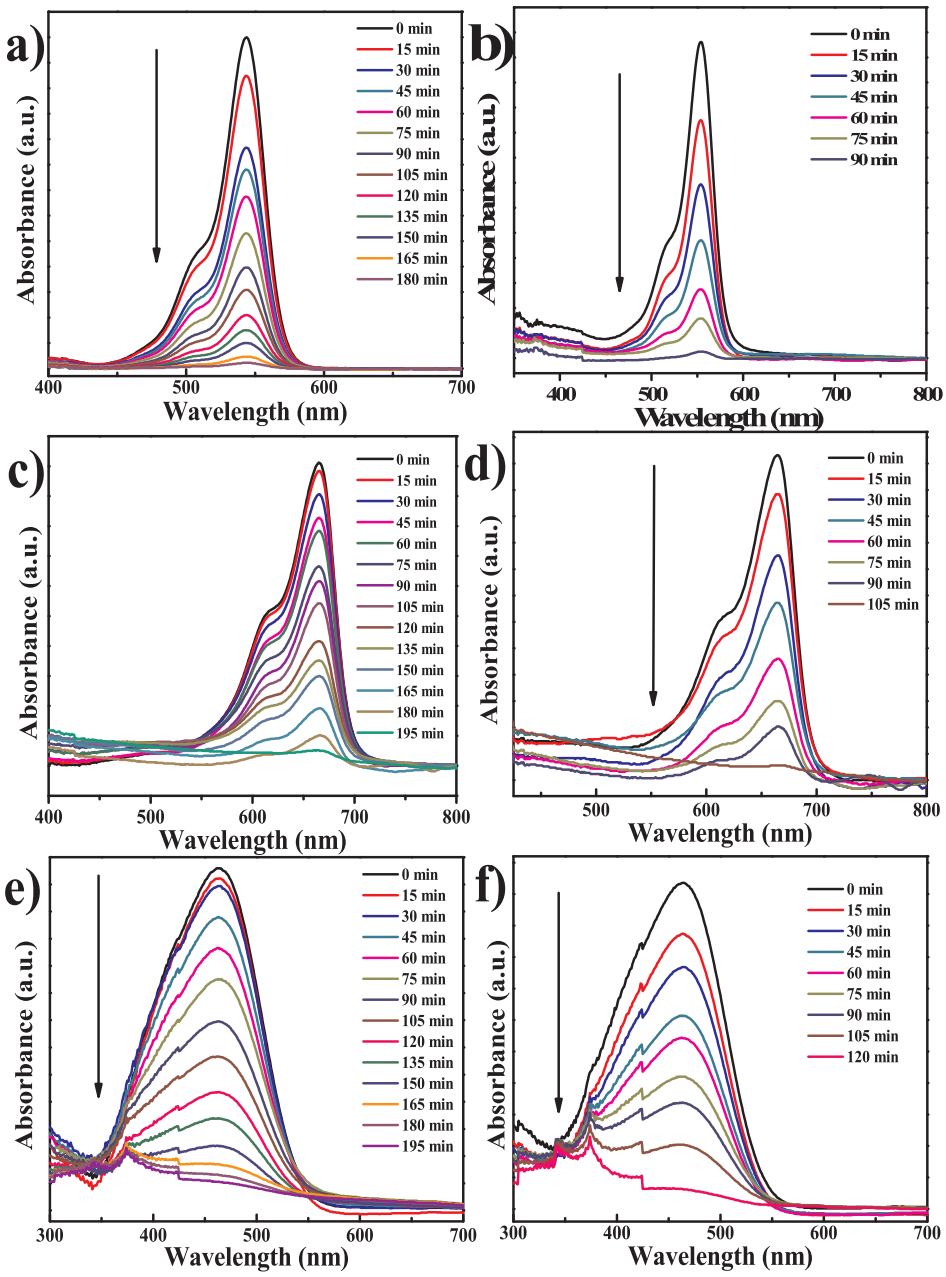

Fig. 8. Time dependent UV–Visible absorption spectra of (a, b) Rh-B, (c, d) MB, (e, f) MO dye solutions in the presence of (a, c and e) ZnO NPs, (b, d and f) G-ZnO NCs.

ZnO-RGO exhibited 73.6% of degradation level upon 80 min visible light irradiation.

Sawant et al. [40] showed that the MO and Rh-B dye molecule degraded up to 96 and 89% after exposing under visible light for 420 min in the presence of ZnO/Gr composite whereas ZnO displayed just 14 and 72% degradation. The Rh-B phtotocatalytic degradation level of the dye molecule was improved from 54.6% (ZnO NPs) to 92.9% using the ZnO/RGO composite after 150 min [41]. Thangavel et al. [42] reported the degradation percentage of MB and Rh-B and showed 42 and 35% for MB and 68 and 55% for MO in 120 min in the presence of ZnO NPs and GD-ZnO NPs respectively. Leng et al. [45] reported that degradation efficiency of ZnO-G nanocomposites towards the methyl orange (MO) dye molecule was 100% after 200 min whereas ZnO showed 79% even after 260 min of irradiation.

A possible mechanism for photocatalytic degradation of dye molecules over G–ZnO nanocomposites is discussed. Upon visible light irradiation, the electrons in the valence band of ZnO NPs can be excited to the conduction band, left holes in the valence band. Then, the photogenerated electrons can be transfer to G due to the interfacial contact between ZnO NPs and G, which hinders the recombination of electrons and holes efficiently. The selected dye molecules can be transferred from the solution to the surface of the nanocomposite and adsorbed with offset face-to face orientation via p–p conjugation between dye molecules and aromatic regions of graphene [15], as evidenced by the enhanced absorptivity of dye molecules over G–ZnO nanocomposites as compared to that over the bare ZnO NPs. The adsorbed dye molecules can be directly oxidized by the hole and the photoactive radicals generated in the photocatalytic reaction produce CO_2, H_2O and other mineralized intermediates.

A novel innovative approach that consists in combining the properties of graphene and ZnO NPs in a freestanding device was presented. This simple assembly method promotes a direct and extensive contact

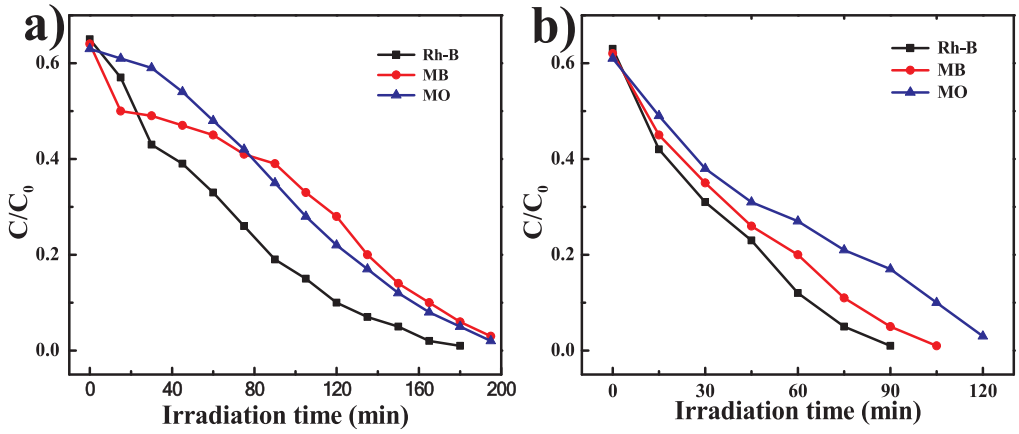

Fig. 9. Photocatalytic degradation of MB, Rh-B and MO in the presence of (a) ZnO NPs and (b) G-ZnO NCs under light irradiation.

Table 1
Comparison of earlier reports with ZnO NPs and G-ZnO NCs for photocatalyst determination of Rh-B, MB and MO dye molecules.

Photocatalyst	Synthesis methods	Dye molecules	Degradation in %		Degradation min		Refs.
			NPs	NCs	NPs	NCs	
ZnO–RGO	Microwave- assisted	MB	41	88	260	260	[21]
Graphene-ZnO	Chemical precipitation	MB	100	100	240	100	[34]
ZnO NP-RGO	Sol-gel	MB	63	99.5	180	180	[26]
ZnO NR-GO	Simultaneous precipitation	MB	41	94	90	90	[37]
		MO	61	83	90	90	
ZnO-RGO	Hydrothermal	MB	64	99.5	130	130	[38]
ZnO- RGO	Microwave-assisted solution	MB	58.7	73.6	80	80	[39]
ZnO/Gr	Electrochemical exfoliation	MO	14	96	420	420	[40]
		Rh-B	47	89	240	240	
ZnO-RGO	Hydrothermal	Rh-B	54.6	92.9	150	150	[41]
GD-ZnO	Hydrothermal	MB	42	68	120	120	[42]
		Rh-B	35	55	120	120	
ZnO-RGO	Electrostatic self-assembly	Rh-B	–	100	–	120	[43]
rGO-ZnO	Hydrolysis -calcination	MO	92	100	150	150	[44]
ZG	Solvothermal technique	MO	79	100	260	200	[45]
G-ZnO	Chemical precipitation	Rh-B	100	100	180	90	Present Work
		MB	100	100	195	105	
		MO	100	100	195	120	

between the graphene and the ZnO NPs through the instauration of non-covalent interactions at the materials interface. At the same time, the NPs coating can confine graphene materials to the direct exposure of light, dyes molecules and OH• radicals, which drastically reduce the photocatalytic efficiencies. On the other hand, the use of sterically hindered cyclic polyporphyrins increases the number of photoactive sites, limiting the formation of agglomerates that hampered the desired charge transfer process at the G-ZnO NCs surface [46].

4. Conclusions

G-ZnO NCs were synthesized using one-step chemical precipitation method and evaluated for the photocatalytic degradation of dye molecules under visible light irradiation. The XRD pattern and Raman spectral analysis confirmed the fabrication of ZnO NPs and G-ZnO NCs. The spherical like ZnO NPs decorated onto the surface of graphene sheets was disclosed by TEM analysis. The G-ZnO NCs showed better photocatalytic efficiency than ZnO NPs against tested dye molecules. The dye degradation level observed was in the order of Rh-B > MB > MO in the presence of G-ZnO NCs. The results suggested that this photodegradation approach could be useful for large scale removal of organic and inorganic pollutants from contaminated waters. It could be concluded that G-ZnO NCs are superior campaigners and could be applied for environmental remediation processes.

Declaration of Competing Interest

The authors declare that they have no known competing financial interests or personal relationships that could have appeared to influence the work reported in this paper.

Acknowledgments

The work was supported by the National Science Foundation of China (NSFC) (Grants 21641007, 21471001), Natural Science Foundation of Anhui Province (Grant no. 1508085), and Major Project of Education Department of Anhui Province (KJ2016SD63). We also thank the Key Laboratory of Environment Friendly Polymer Materials of Anhui Province, and the Postdoctoral Programme, Anhui University, Hefei, Anhui Province, China.

References

[1] B. Li, T. Liu, Y. Wang, Z. Wang, ZnO/graphene-oxide nanocomposite with remarkably enhanced visible-light-driven photocatalytic performance, J. Colloid Interface Sci. 377 (2012) 114–121.
[2] E. Forgacs, T. Cserhati, G. Oros, Removal of synthetic dyes from wastewaters: a review, Environ. Int. 30 (2004) 953–971.
[3] H.S. Rai, M.S. Bhattacharyya, J. Singh, T.K. Bansal, P. Vats, U.C. Banerjee, Removal of dyes from the effluent of textile and dyestuff manufacturing industry: a review of emerging techniques with reference to biological treatment, Crit. Rev. Environ. Sci. Technol. 35 (2005) 219–238.

[4] V.K. Gupta, Suhas, Application of low-cost adsorbents for dye removal - a review, J. Environ. Manage. 90 (2009) 2313–2342.
[5] C.C. Chen, W.H. Ma, J.C. Zhao, Semiconductor-mediated photodegradation of pollutants under visible-light irradiation, Chem. Soc. Rev. 39 (2010) 4206–4219.
[6] M.N. Chong, B. Jin, C.W.K. Chow, C. Saint, Recent developments in photocatalytic water treatment technology: a review, Water Res. 44 (2010) 2997–3027.
[7] J.G. Hou, Z. Wang, S.Q. Jiao, H.M. Zhu, 3D $Bi_{12}TiO_{20}/TiO_2$ hierarchical heterostructure: synthesis and enhanced visible-light photocatalytic activities, J. Hazard. Mater. 192 (2011) 1772–1779.
[8] C. Wang, J. Yan, X. Wua, Y. Song, G. Cai, H. Xu, J. Zhu, H. Li, Synthesis and characterization of $AgBr/AgNbO_3$ composite with enhanced visible-light photocatalytic activity, Appl. Surf. Sci. 273 (2013) 159–166.
[9] T.S. Velayutham, W.H.A. Majid, W.C. Gan, A.K. Zak, S.N. Gan, Theoretical and experimental approach on dielectric properties of ZnO nanoparticles and polyurethane/ZnO nanocomposites, J. Appl. Phys. 112 (2012) 054106.
[10] Z. Chen, N. Zhang, Y.J. Xu, Synthesis of graphene–ZnO nanorod nanocomposites with improved photoactivity and anti-photocorrosion, CrystEngComm. 15 (2013) 3022–3030.
[11] T. Xu, L. Zhang, H. Cheng, Y. Zhu, Significantly enhanced photocatalytic performance of ZnO via graphene hybridization and the mechanism study, Appl. Catal., B 101 (2011) 382–387.
[12] D. Chu, Y. Masuda, T. Ohji, K. Kato, Formation and photocatalytic application of ZnO nanotubes using aqueous solution, Langmuir 26 (2010) 2811–2815.
[13] A.K. Geim, K.S. Novoselov, The rise of graphene, Nat. Mater. 6 (2007) 183–191.
[14] T.N. Lambert, C.A. Chavez, B.H. Sanchez, P. Lu, N.S. Bell, A. Ambrosini, T. Friedman, T.J. Boyle, D.R. Wheeler, D.L. Huber, Synthesis and characterization of titania-graphene nanocomposites, J. Phys. Chem. C 113 (2009) 19812–19823.
[15] H. Zhang, X. Lv, Y. Li, Y. Wang, J. Li, P25-graphene composite as a high performance photocatalyst, ACS Nano 4 (2010) 380–386.
[16] B. Li, H. Cao, ZnO@graphene composite with enhanced performance for the removal of dye from water, J. Mater. Chem. 21 (2011) 3346–3349.
[17] Z.G. Xiong, L.L. Zhang, X.S. Zhao, Visible-light-induced dye degradation over copper-modified reduced graphene oxide, Chem. Eur. J. 17 (2011) 2428–2434.
[18] K.K. Mang, Y. Zhou, Y.L. Yan, K.P. Loh, Multilayer hybrid films consisting of alternating graphene and titania nanosheets with ultrafast electron transfer and photoconversion properties, Adv. Funct. Mater. 19 (2009) 3638–3643.
[19] N.P. Herring, S.H. Almahoudi, C.R. Olson, M.S. El-Shall, Enhanced photocatalytic activity of ZnO–graphene nanocomposites prepared by microwave synthesis, J. Nanopart. Res. 14 (2012) 1277, https://doi.org/10.1007/s11051-012-1277-7.
[20] M. Ahmad, E. Ahmed, Z.L. Honga, J.F. Xu, N.R. Khalid, A. Elhissi, W. Ahmed, A facile one-step approach to synthesizing ZnO/graphene composites for enhanced degradation of methylene blue under visible light, Appl. Surf. Sci. 274 (2013) 273–281.
[21] T. Lv, L. Pan, X. Liu, Z. Sun, Enhanced photocatalytic degradation of methylene blue by ZnO–reduced graphene oxide–carbon nanotube composites synthesized via microwave-assisted reaction, Catal. Sci. Technol. 2 (2012) 2297–2301.
[22] Y. Yang, T. Liu, Fabrication and characterization of graphene oxide/zinc oxide nanorods hybrid, Appl. Surf. Sci. 257 (2011) 8950–8954.
[23] H.-P. Cong, X.-C. Ren, P. Wang, S.-H. Yu, macroscopic multifunctional graphene-based hydrogels and aerogels by a metal ion induced self-assembly process, ACS Nano 6 (2012) 2693–2703.
[24] P. Jayabal, S. Gayathri, V. Sasirekha, J. Mayandi, V. Ramakrishnan, Preparation and characterization of ZnO/graphene nanocomposite for improved photovoltaic performance, J. Nanopart. Res. 16 (2014) 2640, https://doi.org/10.1007/s11051-014-2640-7.
[25] S. Gayathri, P. Jayabal, M. Kottaisamy, V. Ramakrishnan, Synthesis of ZnO decorated graphene nanocomposite for enhanced photocatalytic properties, 173504, J. Appl. Phys. 115 (2014), https://doi.org/10.1063/1.4874877.
[26] W.S. Hummers, R.E. Offeman, Preparation of graphitic oxide, J. Am. Chem. Soc. 80 (1958) 1339–1339.
[27] M. Azarang, A. Shuhaimi, R. Yousefi, A.M. Golsheikh, M. Sookhakian, Synthesis and characterization of ZnO NPs/reduced graphene oxide nanocomposite prepared in gelatin medium as highly efficient photo-degradation of MB, Ceram. Int. 40 (2014) 10217–10221.
[28] L. Zhong, K. Yun, Graphene oxide-modified ZnO particles: synthesis, characterization, and antibacterial properties, Int. J. Nanomed. 10 (2015) 79–92.
[29] Z. Ji, X. Shen, Y. Xu, H. Zhou, S. Bai, G. Zhu, A facile and general route for the synthesis of semiconductor quantum dots on reduced graphene oxide sheets, RSC Adv. 4 (2014) 13601–13609.
[30] J. Lin, M. Penchev, G.P. Wang, R.K. Paul, J.B. Zhong, X.Y. Jing, M. Ozkan, C.S. Ozkan, Heterogeneous graphene nanostructures: ZnO nanostructures grown on large-area graphene layers, Small 6 (2010) 2448–2452.
[31] M. Azarang, A. Shuhaimi, R. Yousefi, M. Sookhakian, Effects of graphene oxide concentration on optical properties of ZnO/RGO nanocomposites and their application to photocurrent generation, 084307, J. Appl. Phys. 116 (2014), https://doi.org/10.1063/1.4894141.
[32] M. Shoeb, B.R. Singh, M. Mobin, G. Afreen, W. Khan, A.H. Naqvi, Kinetic study on mutagenic chemical degradation through three pot synthesiszed Graphene@ZnO nanocomposite, e0135055, PLoS ONE 10 (2015), https://doi.org/10.1371/journal.pone.0135055.
[33] E. Salih, M. Mekawy, R.Y.A. Hassan, I.M. El-Sherbiny, Synthesis, characterization and electrochemical-sensor applications of zinc oxide/graphene oxide nanocomposite, J. Nanostruct. Chem. 6 (2016) 137–144.
[34] Y.L. Chen, Z.A. Hu, Y.Q. Chang, H.W. Wang, Z.Y. Zhang, Y.Y. Yang, H.Y. Wu, Zinc oxide/reduced graphene oxide composites and electrochemical capacitance enhanced by homogeneous incorporation of reduced graphene oxide sheets in zinc oxide matrix, J. Phys. Chem. C 115 (2011) 2563–2571.
[35] G. Milekhin, N.A. Yeryukov, L.L. Sveshnikova, T.A. Duda, E.I. Zenkevich, S.S. Kosolobov, A.V. Latyshev, C. Himcinski, N.V. Surovtsev, S.V. Adichtchev, Z.C. Feng, C.C. Wu, D.S. Wuu, D.R.T. Zahn, Surface enhanced Raman scattering of light by ZnO nanostructures, J. Exp. Theor. Phys. 113 (2011) 983–991.
[36] B. Li, Y. Wang, Facile synthesis and enhanced photocatalytic performance of flower-like ZnO hierarchical microstructures, J. Phys. Chem. C 114 (2010) 890–896.
[37] S.V. Nipane, P.V. Korake, G.S. Gokavin, Graphene-zinc oxide nanorod nanocomposite as photocatalyst for enhanced degradation of dyes under UV light irradiation, Ceram. Int. 41 (2015) 4549–4557.
[38] X. Zhou, T. Shi, H. Zhou, Hydrothermal preparation of ZnO-reduced graphene oxide hybrid with high performance in photocatalytic degradation, Appl. Surf. Sci. 258 (2012) 6204–6211.
[39] F.S. Omar, H.N. Ming, S.M. Hafiz, L.H. Ngee, Microwave synthesis of Zinc oxide/reduced graphene oxide hybrid for adsorption-photocatalysis application, Int. J. Photoenergy (2014) Article ID 176835. doi:10.1155/2014/176835.
[40] S.Y. Sawant, M.H. Cho, Facile electrochemical assisted synthesis of ZnO/graphene nanosheets with enhanced photocatalytic activity, RSC Adv. 5 (2015) 97788–97797.
[41] X. Li, Q. Wang, Y. Zhao, W. Wu, J. Chen, H. Meng, Green synthesis and photocatalytic performances for ZnO-reduced graphene oxide nanocomposites, J. Colloid Interface Sci. 411 (2013) 69–75.
[42] S. Thangavel, K. Krishnamoorthy, V. Krishnaswamy, N. Raju, S.J. Kim, G. Venugopal, Graphdiyne−ZnO nanohybrids as an advanced photocatalytic material, J. Phys. Chem. C 119 (2015) 22057–22065.
[43] B. Weng, M.-Q. Yang, N. Zhang, Y.-J. Xu, Toward the enhanced photoactivity and photostability of ZnO nanospheres via intimate surface coating with reduced graphene oxide, J. Mater. Chem. A 2 (2014) 9380–9389.
[44] J. He, C. Niu, C. Yang, J. Wanga, X. Su, Reduced graphene oxide anchored with zinc oxide nanoparticles with enhanced photocatalytic activity and gas sensing properties, RSC Adv. 4 (2014) 60253–60259.
[45] Y. Leng, W. Wang, L. Zhang, F. Zabihi, Y. Zhao, Fabrication and photocatalytical enhancement of ZnO-graphene hybrid using a continuous solvothermal technique, J. Supercrit. Fluids 91 (2014) 61–67.
[46] Z. Chen, N. Zhang, Y.-J. Xu, Synthesis of graphene–ZnO nanorod nanocomposites improved photoactivity and anti-photocorrosion, CrystEngComm 15 (2013) 3022–3030.